LOW-VOLTAGE RIDE-THROUGH CAPABILITY FOR DFIG WIND TURBINE SYSTEM BASED ON SERIES GRID-SIDE CONVERTER

Van Tan Luong[*], Nhut Minh Ho[+]
[*] Ho Chi Minh city University of Industry and Trade
[+] Posts and Telecommunications Institute of Technology

Abstract - This paper proposes a low-voltage ride-through (LVRT) capability for a doubly-fed induction generator (DFIG) wind turbine (WT) system. With the proposed method, series grid-side converter (SGSC) in which its DC-side connected at the DC bus of the back-to-back converters and its AC-side connected in series with line through transformer have been applied, enables to compensate a voltage response of the system during the grid faults and to reduce the capital cost. A control algorithm for SGSC consisting of both positive- sequence component voltage controllers based on sliding mode control (SMC) and negative - sequence component voltage controllers based on proportional integral (PI) control is performed in the dq synchronous reference frame. Also, to protect the DC capacitor from its overvoltage, a braking chopper has been employed. The simulation results for 2 MW-DFIG wind turbine system with the voltage compensation at the grid faults are presented, give as good performance as those without grid faults.

Keywords - Doubly-fed induction generator, low-voltage ride-through, series voltage-source converter, voltage sag, wind turbine.

I. INTRODUCTION

In recent years, renewable energy has been paid a considerable attention, since the fossil fuels are being exhausted and environmental issues have become more seriously. Wind energy is considered as one of the most important renewable energy sources, where the significant penetration of wind power capacity may cause some problems in the power system such as grid instability, unbalance, and frequency variation [1]- [2].

A doubly fed induction generator (DFIG) is a common subsystem for large variable speed wind turbines in which the stator windings are directly connected to the grid and the rotor windings are served as a power interface between the rotor windings and the grid through by back-to-back pulse-width modulation (PWM) converter. The power rating of the back-to-back converter is typically designed as 30% of nominal rating of the wind turbine and mainly depends on the speed operation range of the DFIG. Thus, deep voltage sags and the stator flux cause a considerable electrical stress on the rotor-side converter and thereby increase mechanical stress on the gearbox as well [1 - 2].

The grid codes require a low-voltage ride-through (LVRT) capability of the wind turbine system. For several national grid codes, the wind power systems should stay connected to the grid for the grid fault conditions, as illustrated in Figure 1 [3].

To improve the fault handling capacity and protect the DFIG converter from high rotor current during grid faults, a crowbar is usually adopted to limit the high rotor currents and rotor voltages [4]-[12]. In [11], the behavior of DFIG and the low voltage ride through capability have been investigated, when an active crowbar is connected between the rotor side of the DFIG and the rotor-side converter (RSC) by short-circuiting the rotor temporarily. It was found that DFIG allows the reactive support to the power grid during both the normal and grid fault conditions, and this support is relatively larger when a voltage controller is used and the wind generator operates with the light load, instead of constant power factor control of the DFIG. Also, a strategy of the coordinated crowbar and braking chopper is suggested to reduce undesirable fault effects by contributing to the grid voltage control during the grid fault [12]. The crowbar technology and the braking resistor do not fulfill the grid codes during the duration of the activation of the braking resistor or the crowbar. To satisfy the grid codes, static synchronous compensator (STATCOM) and dynamic voltage restorer (DVR) to enhance the ride-through capability of wind turbines or wind farms [13] – [20]. STATCOM, known as shunt voltage compensation, is connected in parallel to the line, while DVR, referred as series voltage compensation, is connected in series with the line via the transformer. However, STATCOM can not cope with deep voltage fault since it is based on shunt compensation. Meanwhile, DVR, a series compensator, would be much more effective to restore voltage in strong grid utility. Nevertheless, the

Contact author: Van Tan Luong
Email: luonghepc@gmail.com
Manuscript received: 6/2023, revised: 7/2023, accepted: 8/2023.

cost of the DVR is so high to solve this problem practically.

In this paper, the application of a series grid-side converter (SGSC) that is connected to a wind-turbine-driven DFIG system to allow uninterruptible fault ride-through capability of voltage dips fulfilling the grid code requirements is investigated. With the proposed method, DC-side of SGSC is connected to the DC bus of the back-to-back converters, instead of using an additional diode rectifier, while its AC-side is connected in series with line through transformer. Thus, this can reduce the capital cost, instead of using an expensive DVR. Also, for SGSC control, a positive- sequence component voltage controllers based on sliding mode control (SMC) and negative - sequence component voltage controllers based on proportional integral (PI) control are performed in the dq synchronous reference frame, from which the SGSC can compensate the faulty line voltage well. Simulation results for a 2 MW-DFIG wind turbine system are provided, gives as good performance as those without grid faults.

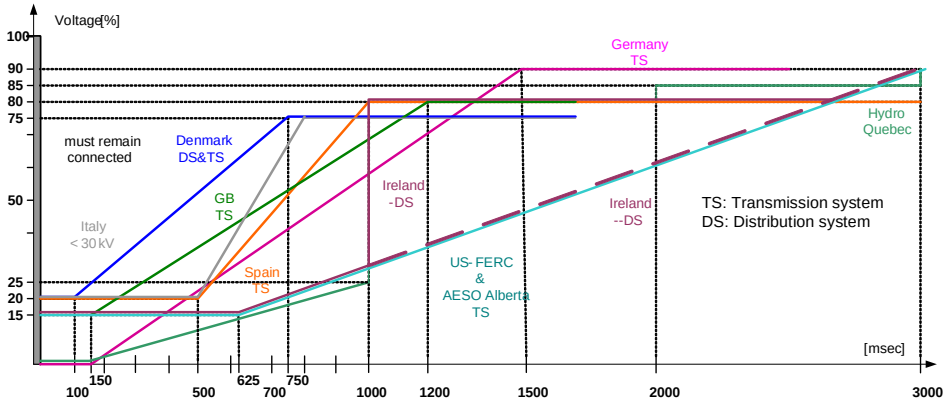

Figure 1. National grid codes [3].

II. SYSTEM MODELING

A single-line schematic of the DFIG with SGSC is shown in Figure 2. As can be seen in a conventional DFIG, the rotor windings of the machine are accessed via slip rings and connected to a three-phase converter referred to as RSC. The RSC shares a DC bus with a second converter connected in parallel with the grid and DFIG stator, referred to as the grid-side converter (GSC). The shared DC link enables power to flow between the rotor circuit of the DFIG and the grid connection. The proposed topology includes an additional converter connected in series with the line through transformer, known as SGSC. Also, a braking chopper added to DC bus is to keep the DC-link voltage at its rated value.

The modeling of the SGSC is briefly described in this section, in which the components of the positive and negative-sequence currents and voltages of the SGSC can be expressed in synchronous d-q reference frame as follows [16]-[17]:

$$\begin{cases} \dot{V}_{cq}^{+} = \dfrac{1}{C} I_{fq}^{+} - \omega_e \dfrac{C_f}{C} V_{cd}^{+} - \dfrac{1}{C} I_{sq}^{+} \\ \dot{I}_{fq}^{+} = \dfrac{1}{L_f} V_{fq}^{+} - \omega_e I_{fd}^{+} - \dfrac{1}{L_f} V_{cq}^{+} \\ \dot{V}_{cd}^{+} = \dfrac{1}{C} I_{fd}^{+} + \omega_e \dfrac{C_f}{C} V_{cq}^{+} - \dfrac{1}{C} I_{sd}^{+} \\ \dot{I}_{fd}^{+} = \dfrac{1}{L_f} V_{fd}^{+} + \omega_e I_{fq}^{+} - \dfrac{1}{L_f} V_{cd}^{+} \end{cases} \quad (1)$$

$$\begin{cases} \dot{V}_{cq}^{-} = \dfrac{1}{C} I_{fq}^{-} + \omega_e \dfrac{C_f}{C} V_{cd}^{-} - \dfrac{1}{C} I_{sq}^{-} \\ \dot{I}_{fq}^{-} = \dfrac{1}{L_f} V_{fq}^{-} + \omega_e I_{fd}^{-} - \dfrac{1}{L_f} V_{cq}^{-} \\ \dot{V}_{cd}^{-} = \dfrac{1}{C} I_{fd}^{-} - \omega_e \dfrac{C_f}{C} V_{cq}^{-} - \dfrac{1}{C} I_{sd}^{-} \\ \dot{I}_{fd}^{-} = \dfrac{1}{L_f} V_{fd}^{-} - \omega_e I_{fq}^{-} - \dfrac{1}{L_f} V_{cd}^{-} \end{cases} \quad (2)$$

where V_{cd}^{+}, V_{cq}^{+}, V_{cd}^{-}, and V_{cq}^{-} are the dq-components of the voltage across the filter capacitor of the SGSC. V_{fd}^{+}, V_{fq}^{+}, V_{fd}^{-}, and V_{fq}^{-} are the dq-components of the inverter output voltage of the SGSC. I_{sd}^{+}, I_{sq}^{+}, I_{sd}^{-}, and I_{sq}^{-} are dq components of the grid current. I_{fd}^{+}, I_{fq}^{+}, I_{fd}^{-}, and I_{fq}^{-} are dq-components of the filter inductor current of the SGSC. It is noted that the subscripts "+" and "-" denote the positive and negative-sequence components, respectively.

From (1), a state-space modeling of the system written in the positive sequence-components is derived as follows:

$$\begin{bmatrix} \dot{V}_{cq}^{+} \\ \dot{I}_{fq}^{+} \\ \dot{V}_{cd}^{+} \\ \dot{I}_{fd}^{+} \end{bmatrix} = \begin{bmatrix} 0 & 0 & -\frac{\omega_e C_f}{C} & 0 \\ -\frac{1}{L_f} & 0 & 0 & 0 \\ \frac{\omega_e C_f}{C} & 0 & 0 & 0 \\ 0 & 0 & -\frac{1}{L_f} & 0 \end{bmatrix} \begin{bmatrix} V_{cq}^{+} \\ I_{fq}^{+} \\ V_{cd}^{+} \\ I_{fd}^{+} \end{bmatrix} + \begin{bmatrix} 0 & 0 \\ \frac{1}{L_f} & 0 \\ 0 & 0 \\ 0 & \frac{1}{L_f} \end{bmatrix} \begin{bmatrix} V_{fq}^{+} \\ V_{fd}^{+} \end{bmatrix} + \begin{bmatrix} -\frac{1}{C} I_{sq}^{+} \\ 0 \\ -\frac{1}{C} I_{sd}^{+} \\ 0 \end{bmatrix} \quad (3)$$

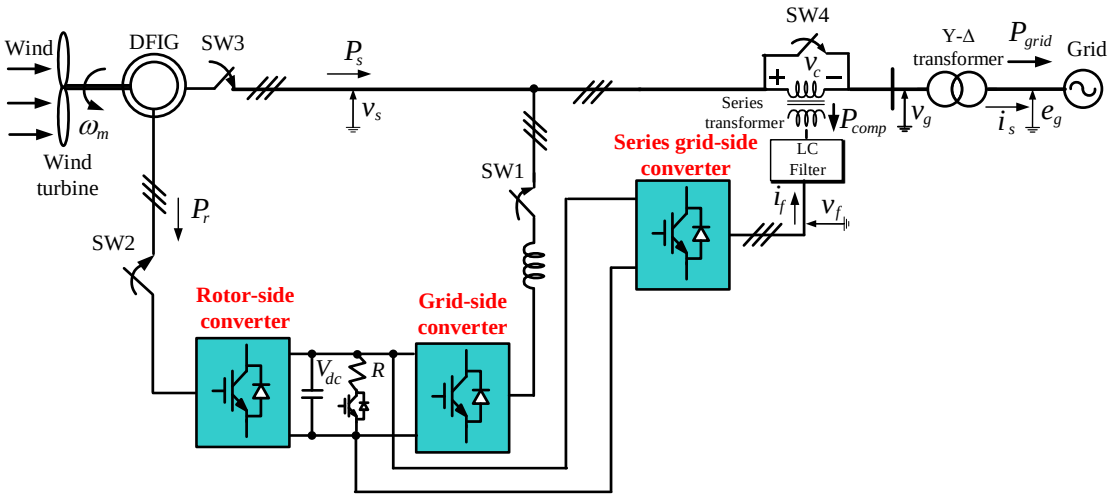

Figure 2. DFIG wind turbine system with SGSC and braking chopper.

III. PROPOSED CONTROL

A. Compensation of voltage sag

The reference of the compensation voltage across the series transformer injected by the SGSC can be expressed as:

$$\begin{bmatrix} v_{ca}^{*} \\ v_{cb}^{*} \\ v_{cc}^{*} \end{bmatrix} = \begin{bmatrix} v_{ga,presag} - v_{ga} \\ v_{gb,presag} - v_{gb} \\ v_{gc,presag} - v_{gc} \end{bmatrix} \quad (4)$$

where $v_{ga,presag}$, $v_{gb,presag}$ and $v_{gc,presag}$ are the voltages across the low-voltage side of the Y/Δ transformer before the sag; v_{ga}, v_{gb} and v_{gc} are the voltages after the sag.

B. Control of SGSC using sliding mode control

A multi-input multi-output (MIMO) nonlinear approach is proposed for the purpose of eliminating the nonlinearity in the modeled system [18]-[21]. A multi-input multiple-output system can be considered as:

$$\dot{x} = f(x) + gu \quad (5)$$

$$y = h(x) \quad (6)$$

where x is the state vector, u is the control input, y is the output, f and g are the smooth vector fields, respectively, and h is the smooth scalar function.

The nonlinear model of the SGSC in (3) is expressed in (5) and (6) as:

$x = \begin{bmatrix} V_{cq}^{+} & I_{fq}^{+} & V_{cd}^{+} & I_{fd}^{+} \end{bmatrix}^T$; $u = \begin{bmatrix} V_{fq}^{+} & V_{fd}^{+} \end{bmatrix}^T$; $y = \begin{bmatrix} V_{cq}^{+} & V_{cd}^{+} \end{bmatrix}^T$ To generate an explicit relationship between the outputs $y_{i=1,2}$ and the inputs $u_{i=1,2}$, each output is differentiated until a control input appears.

$$\begin{bmatrix} \ddot{y}_1 \\ \ddot{y}_2 \end{bmatrix} = \begin{bmatrix} v_1 \\ v_2 \end{bmatrix} = A(x) + E(x) \begin{bmatrix} u_1 \\ u_2 \end{bmatrix} \quad (7)$$

Then, the control law is given as

$$\begin{bmatrix} V_{fq}^{*} \\ V_{fd}^{*} \end{bmatrix} = \begin{bmatrix} u_1 \\ u_2 \end{bmatrix} = E^{-1}(x) \left[-A(x) + \begin{bmatrix} v_1 \\ v_2 \end{bmatrix} \right] \quad (8)$$

Where

$$A(x)=\begin{bmatrix} \frac{\omega_e}{C}\left(1+\frac{C_f}{C}\right)I_{fd}^{+}+\frac{1}{C}\left(\frac{1}{L_f}+\frac{\omega_e^2C_f^2}{C}\right)V_{cq}^{+}+\frac{1}{C}\dot{I}_{sq}^{+}-\frac{\omega_eC_f}{C^2}I_{sd}^{+} \\ -\frac{\omega_e}{C}\left(1+\frac{C_f}{C}\right)I_{fq}^{+}+\frac{1}{C}\left(\frac{1}{L_f}+\frac{\omega_e^2C_f^2}{C}\right)V_{cd}^{+}+\frac{1}{C}\dot{I}_{sd}^{+}+\frac{\omega_eC_f}{C^2}I_{sq}^{+} \end{bmatrix};\quad E^{-1}(x)=\begin{bmatrix} L_fC & 0 \\ 0 & L_fC \end{bmatrix}$$

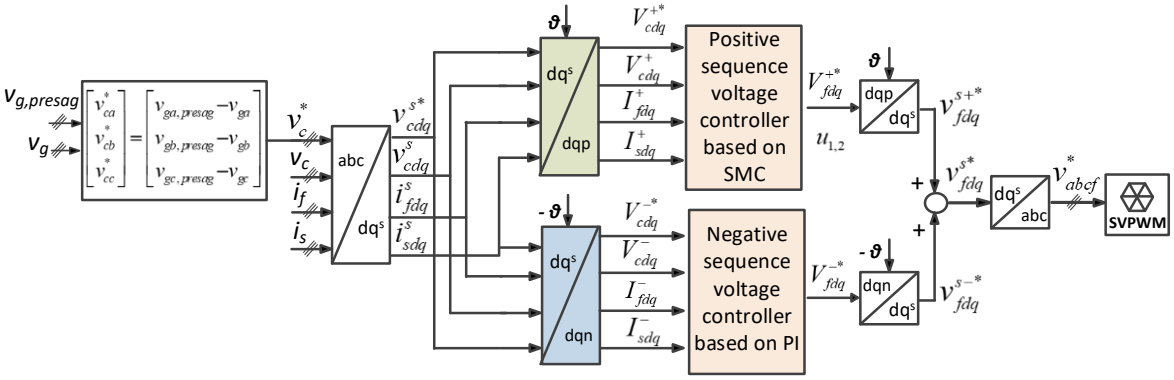

Figure 3. Voltage control block diagram of SGSC

By using a sliding mode control theory, the equivalent control input can be derived as the continuous control input that $\dot{s}_1=\dot{s}_2=0$ yields.

$$\begin{bmatrix} u_{1eq} \\ u_{2eq} \end{bmatrix}=\begin{bmatrix} L_fC\left[v_1+H_{11}+H_{12}\right] \\ L_fC\left[v_2+H_{21}+H_{22}\right] \end{bmatrix} \qquad (10)$$

Where

$$H_{11}=\frac{\omega_e}{C}\left(1+\frac{C_f}{C}\right)I_{fd}^{+}+\frac{1}{C}\left(\frac{1}{L_f}+\frac{\omega_e^2C_f^2}{C}\right)V_{cq}^{+}$$

$$H_{21}=-\frac{\omega_e}{C}\left(1+\frac{C_f}{C}\right)I_{fq}^{+}+\frac{1}{C}\left(\frac{1}{L_f}+\frac{\omega_e^2C_f^2}{C}\right)V_{cd}^{+}$$

$$H_{12}=\frac{1}{C}\dot{I}_{sq}^{+}-\frac{\omega_eC_f}{C^2}I_{sd}^{+}$$

$$H_{22}=\frac{1}{C}\dot{I}_{sd}^{+}+\frac{\omega_eC_f}{C^2}I_{sq}^{+}$$

To drive the state variables to the sliding surface $s_1=s_2=0$, in the case of $s_1\neq 0, s_2\neq 0$, the control laws are defined as

$$\begin{aligned} u_1&=u_{1eq}+\mu_1 sign(s_1) \\ u_2&=u_{2eq}+\mu_2 sign(s_2) \end{aligned} \qquad (11)$$

where $\mu_1>0$, $\mu_2>0$.

The reaching law can be derived by substituting (11) into (9), which gives.

$$\dot{s}_1=-\mu_1 sign(s_1);\quad \dot{s}_2=-\mu_2 sign(s_2) \qquad (12)$$

In order to determine the stability and robustness, Lyapunov's functions which are presented in [21].

The block diagram of the proposed control is shown in Figure 3, whereas the components of the positive-sequence voltages in the dq-axis are separately controlled by using the SMC. Meanwhile, the components of the negative-sequence voltages in the dq-axis are regulated, depending on the PI controller [17]. Then, the outputs of the SMC control ($u_{12}=V_{fdq}^{+*}$) and the PI control (V_{fdq}^{-*}) are transformed to the voltage references in three-phase abc reference frame, applied for the space vector pulse-width modulation (SVPWM) [22].

IV. SIMULATION RESULTS

To verify the feasibility of the proposed method, PSCAD simulation has been carried out for a 2 MW-DFIG wind turbine system. The parameters of the wind turbine, generator and series grid-side converter are listed in Table 1, 2 and 3, respectively.

Table 1. Parameters of wind turbine

Parameter	Value
Rated power	2 MW
Blade radius	45 m
Air density	1.225 kg/m^3
Max. power conv. coefficient	0.4
Cut-in speed	3 m/s
Cut-out speed	25 m/s
Rated wind speed	16.5 m/s
Blade inertia	6.3x10^6 kg.m^2

Table 2. Parameters of 2 MW- DFIG

Parameter	Value
Rated power	2 MW
Grid voltage	690 V
Stator voltage/frequency	690 V/60 Hz
Stator resistance	0.00488 pu
Rotor resistance	0.00549 pu
Stator leakage inductance	0.0924 pu
Rotor leakage inductance	0.0995 pu
Generator inertia	200 kg.m2

Table 3. Parameters of SGSC

Parameter	Value
Capacity	0.8 MW
DC-link capacitor	8200 μF
Inverter output filter	L=0.1 mH, C =1000 μF
Switching frequency	2.5 kHz
Series transformer	0.8 MW, 690 V/ 690 V

Figure 4 shows the system performance for unbalanced grid voltage fault without using SGSC system, where the wind speed is assumed to be constant (16.5 m/s) for easy investigation. The fault condition is 50% sag in phases A and B for 0.1 s which is between 1.6 s and 1.7 s. When there is the grid unbalanced voltage sag (V_{gabc}) as shown in Figure 4(a), the negative-sequence component of the grid voltage exist. As can be seen from Figure 4 (b), the DC-link voltage (V_{dc}) of the DFIG converter without using SGSC reaches 2.9 pu, which can destroy the DC capacitor and the switches of the converter. Also, the stator and rotor currents (i_{abcs}, i_{abcr}) are increased, as illustrated in Figure 4(c) to 4(d), respectively. In this case, the generator speed (ω_r), as illustrated in Figure 4(e) accelerates to obtain the optimal value for tracking the maximum power point. Similarly, the generator torque (T_g)in Figure 4(f) is also oscillated under the grid voltage fault.

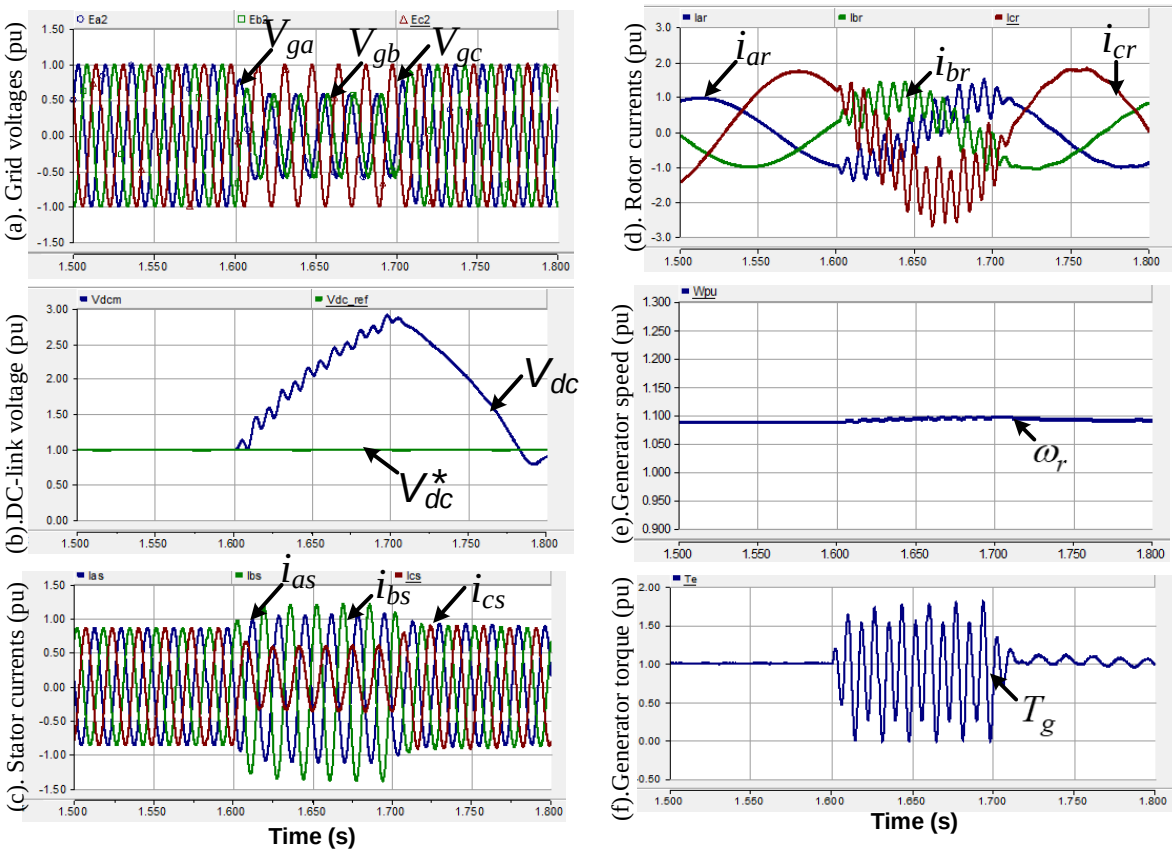

Figure 4. Performance of DFIG wind turbine system for unbalanced voltage sag (in pu). (a) Grid voltages. (b) DC-link voltage. (c) Stator power. (d) Rotor power. (e) Stator currents. (f) Rotor currents. (g). Generator speed. (h) Generator torque.

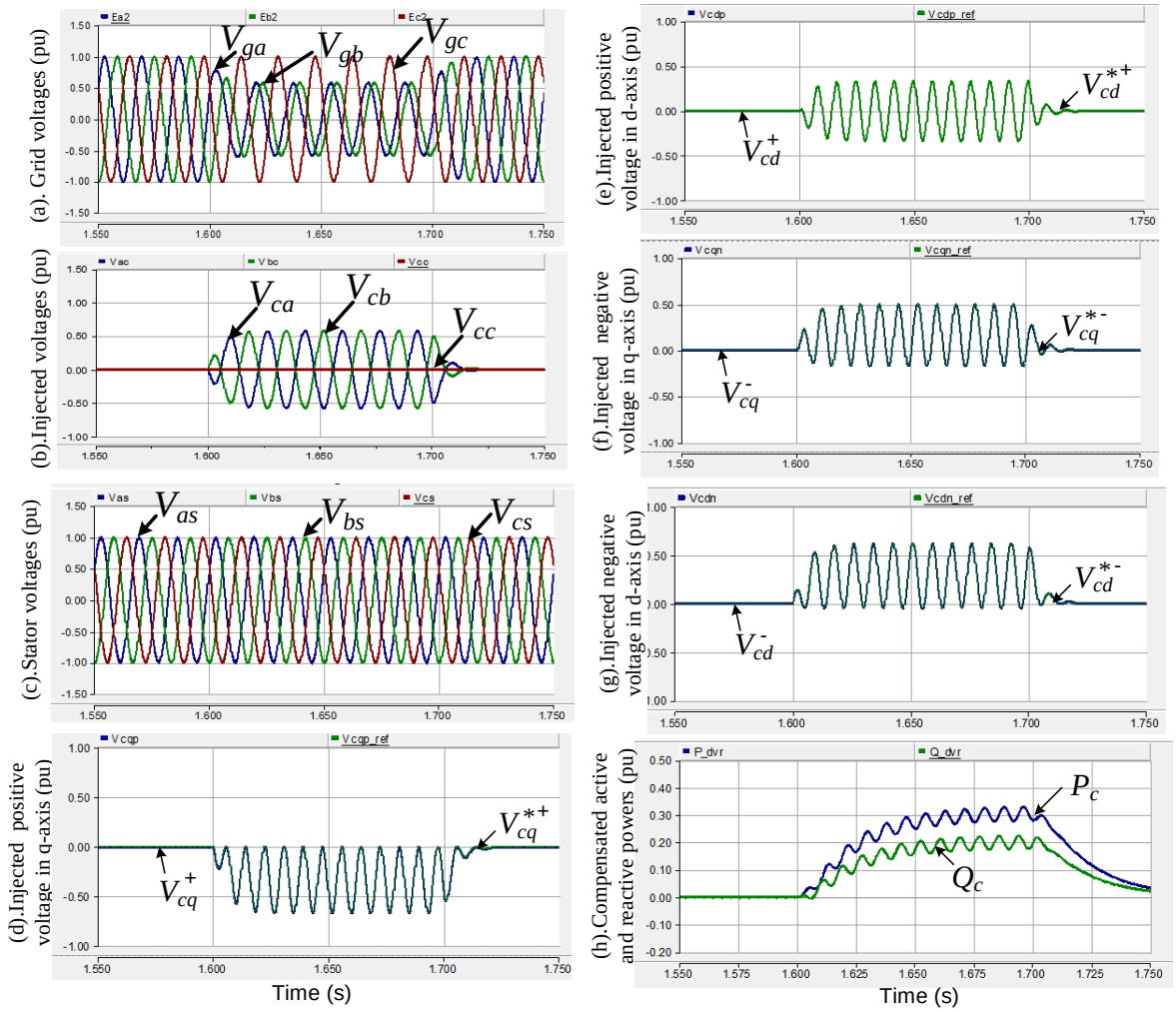

Figure 5. Performance of series volatge-source converter system for unbalanced voltage sag (in pu). (a) Grid voltages. (b) SGSC output voltages. (c) Stator voltages. (d) q-axis positive voltages of SVSC. (e) d-axis positive voltages of SGSC. (f) q-axis negative voltages of SGSC. (g) d-axis negative voltages of SGSC. (h) Compensated active and reactive powers.

Figure 5 shows the performance of SGSC system under balanced grid voltage fault. Due to unbalanced voltage sag, as shown in Figure 5 (a), the compensation voltages (V_{cabc}) in Figure 5 (b) are injected by the SGSC system. With the compensation, the stator voltages (V_{abcs}) in Figure 5 (c) compensated, are kept at the rated value. The dq-axis voltages (V_{cdq}) of the SGSC are shown from Figure 5 (d) and (e), respectively. Aslo, the active and reactive powers (P_c , Q_c) injected by the SGSC are shown in Figure 5 (f). Without SGSC for voltage compensation, the stator and rotor currents, and generator torque give high oscillations, as seen in Figure 4(c), 4(d) and 4(f), respectively. However, they are kept almost constant with compensation.

Figure 6 shows the performance of DFIG wind turbine system under unbalanced voltage fault. It is clear from Figure 6 that all quantities of the DFIG with the proposed SGSC such as DC-link voltage, stator active and reactive powers, stator and rotor currents, generator speed and torque during grid faults have the same waveforms as those without grid faults. On the other hand, the DFIG still operates normally as if the grid fault occurs. Thus, the proposed method obtains the better operation for the DFIG wind turbine system during asymmetrical grid fault. Also, the proposed method can satisfy with almost all national grid codes. On the other hands, the wind power systems still maintain connected to the grid under the grid fault conditions, as shown in Figure 1.

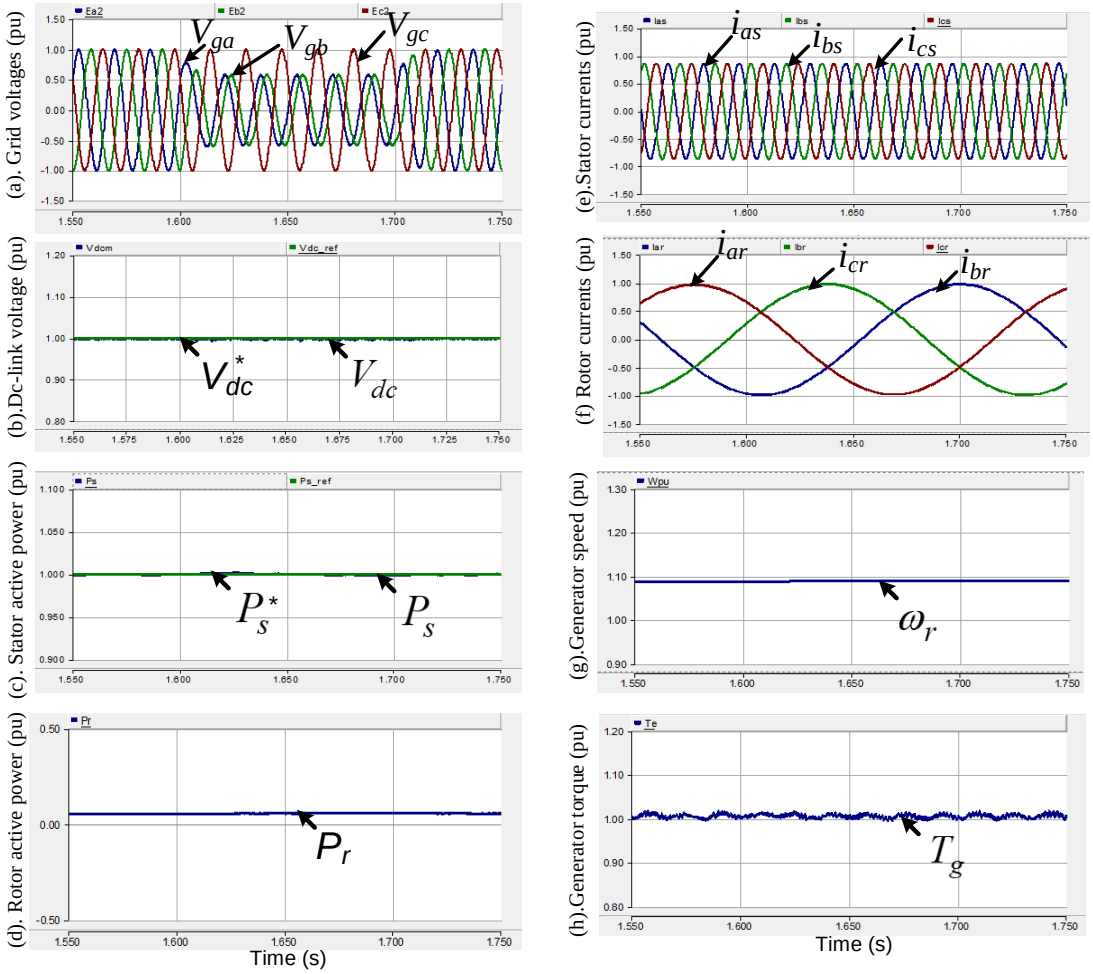

Figure 6. Performance of DFIG wind turbine system for unbalanced voltage sag (in pu). (a) Grid voltages. (b) DC-link voltage. (c) Stator active power. (d) Stator reactive power. (e) Stator current. (f) Rotor current. (g) Generator speed. (h) Generator torque.

V. CONCLUSION

In this paper, the application of a SGSC connected to a wind-turbine-driven DFIG to allow uninterruptible fault ride through of grid voltage faults is introduced. With the proposed method, the DC-side of the SGSC is connected at the DC bus of the back-to-back converters without using diode rectifier, and thus reduce the capital cost. For SGSC control, positive- and negative-sequence component voltage controllers which are respectively based on SMC and PI control are performed in the dq synchronous reference frame. Also, to prevent the DC capacitor from its overvoltage, a braking chopper has been employed. The simulation results for 2 MW-DFIG wind turbine system with the voltage compensation at the grid faults are presented, give as good performance as those without grid faults.

REFERENCES

1. Anaya-Lara O., Wu X., Cartwright P., Ekanayake J. B., and Jenkins N. (2005), "Performance of doubly fed induction generator (DFIG) during network faults", Wind Engineering, Vol. 29, No. 1, pp. 49–66.
2. Polinder H., van der Pijl F. F. A., de Vilder G. J., and Tavner P. J. A. T. P. J. (2006), "Comparison of direct-drive and geared generator concepts for wind turbines", IEEE Transactions on Energy Conversion, Vol. 21, No. 3, pp. 725–733.
3. Iov F., Hansen A.D., Sørensen P., and Cutululis N. A (2007)., "Mapping of grid faults and grid codes", Technical Report Risø-R-1617(EN), Risø National Laboratory, Technical University of Denmark, Roskilde, Denmark.
4. Morren J. and de Haan S. W. H. (2005), "Ridethrough of wind turbines with doubly-fed induction generator during a voltage dip", IEEE Transactions on Energy Conversion, Vol. 20, No. 2, pp. 435–441.
5. Dittrich A. and Stoev A. (2005), "Comparison of fault ride-through for wind turbines with DFIM generators", in Proceedings 11th European Conference Power Electronics Applications, pp. 1–8.
6. Causebrook A., Atkinson D. J., and Jack A. G. (2007), "Fault ride-through of large wind farms using series dynamic braking resistors", IEEE Transactions on Power System, Vol. 22, No. 3,

pp. 966–975.

7. Morren J. and de Haan S. W. H. (2005), "Ride-through of wind turbines with doubly-fed induction generator during a voltage dip", IEEE Transactions on Energy Conversion, Vol. 20, No. 2, pp. 435–441.
8. Gomis-Bellmunt O., Junyent-Ferre A., Sumper A., and Bergas-Jan J. (2008), "Ride-through control of a doubly fed induction generator under unbalanced voltage sags", IEEE Transactions on Energy Conversion, Vol. 23, No. 4, pp. 1036–1045.
9. Peng L., Francois B., and Li Y. (2009), "Improved crowbar control strategy of DFIG based wind turbines for grid fault ride-through", in Proceedings IEEE 24th Annual Applied on Power Electronics Conference and Exposition, pp.1932-1938.
10. Zhou P. and He Y. (2007), "Control strategy of an active crowbar for DFIG based wind turbine under grid voltage dips", in Proceedings International Conference on Electrical Machines and Systems, pp. 259–264.
11. G. Tsourakis, C. D. Vournas (2006), "Simulation of low voltage ride through capability of wind turbines with doubly fed induction generator," in Proc. European Wind Energy conference.
12. Haidar A. M. A., Muttaqi K. M., and Hagh M. T. (2017), "A coordinated control approach for DC link and rotor crowbars to improve fault ride-through of DFIG based wind turbines", IEEE Transactions Industry Applications, Vol. 53, No. 4, pp. 4073-4086.
13. Abdel-Baqi O. and Nasiri A. (2010), "A dynamic LVRT solution for doubly-fed induction generators", *IEEE Transactions on Power Electronics*, Vol. 25, No. 1, pp.193–196.
14. Luo J., Zhao H., Lu X., Gao S., Ma Q. , and Terzija V. (2019), "A Review of Low Voltage Ride Through in DFIG under Unbalanced Grid Faults", 2019 IEEE PES GTD Grand International Conference and Exposition Asia (GTD Asia), pp. 718-723.
15. Nguyen T. H. , Lee D. C., Van T. L., and Kang J.-H. (2013), "Coordinated Control of Reactive Power between STATCOMs and Wind Farms for PCC Voltage Regulation", Journal of Power Electronics, Vol. 13, No. 5, pp. 909-918.
16. Van T. L. and Ho V. C. (2015), "Enhanced Fault Ride-Through Capability of DFIG Wind Turbine Systems Considering Grid-Side Converter as STATCOM", Lecture notes in electrical engineering, Vol. 371, pp. 185-196.
17. Ibrahim A. O., Nguyen T. H., Lee D.-C., and Kim S.-C. (2011), "A fault ridethrough technique of DFIG wind turbine systems using dynamic voltage restorers", IEEE Transactions on Energy Conversion, Vol. 26, No. 3, pp. 871–882.
18. Van T. L., Nguyen N. M. D., Toi L. T. and Trang T. T. (2017). "Advanced Control Strategy of Dynamic Voltage Restorers for Distribution System Using Sliding Mode Control Input-Ouput Feedback Linearization", Lecture notes in electrical engineering, Vol. 465, pp. 521-531.
19. Awad H., Svensson J., and Bollen M. (2004), "Mitigation of unbalanced voltage dips using static series compensator", IEEE Transactions on Power Electronics, Vol. 19, No. 3, pp. 837–846.
20. Kim M.-B., Moon G.-W., and Youn M.-J. (2004), "Synchronous PI decoupling control scheme for dynamic voltage restorer against a voltage sag in the power system", in Proceedings of Annual IEEE Conference on Power Electronics Specialists, Vol. 2, pp. 1046–1051.
21. Slotine J.-J. E. and Li W. (1991), Applied Nonlinear Control. Englewood Cliffs, NJ: Prentice-Hall, pp. 207–271.
22. Kim J.-S. and Sul S.-K. (1996), "A Novel Voltage Modulation Technique of the Space Vector PWM", Transactions on IEE Japan, Vol. 116-D, No. 8, pp. 820 – 825.

KHẢ NĂNG LƯỚT QUA ĐIỆN ÁP THẤP CỦA HỆ THỐNG TUA BIN GIÓ DFIG DỰA VÀO BỘ BIẾN ĐỔI PHÍA LƯỚI NỐI TIẾP

Tóm tắt: Bài báo đề xuất khả năng lướt qua điện áp thấp (LVRT) của hệ thống tua bin gió dùng DFIG. Với phương pháp được đề xuất, phía DC của bộ chuyển đổi phía lưới nối tiếp (SGSC) được kết nối với thanh cái DC của các bộ chuyển đổi back-to-back và phía AC của nó được kết nối nối tiếp với đường dây qua máy biến áp và bộ SGSC có khả năng bù đáp ứng điện áp của hệ thống trong thời gian xảy ra sự cố lưới điện và giảm chi phí vốn đầu tư. Thuật toán điều khiển cho SGSC bao gồm cả bộ điều khiển điện áp thành phần thứ tự thuận dựa trên điều khiển chế độ trượt (SMC) và bộ điều khiển điện áp thành phần thứ tự nghịch dựa trên điều khiển tích phân tỷ lệ (PI) được thực hiện trong hệ quy chiếu đồng bộ dq. Ngoài ra, để bảo vệ tụ điện DC khỏi quá áp của nó, braking chopper đã được sử dụng. Kết quả mô phỏng cho hệ thống tua bin gió 2 MW-DFIG có bù điện áp khi có sự cố lưới điện được trình bày, cho kết quả vận hành tốt, như trong trường hợp hệ thống không có sự cố lưới.

Từ khóa **–** máy phát không đồng bộ nguồn kép, lướt qua điện áp thấp, bộ chuyển đổi phía lưới nối tiếp, sụt áp, tua bin gió.

Van Tan Luong was born in Vietnam. He received the B.Sc. and M.Sc. degrees in electrical engineering from Ho Chi Minh City University of Technology, Ho Chi Minh city, Vietnam, in 2003 and 2005, respectively, and Ph.D. degree in electrical engineering from Yeungnam University, Gyeongsan, South Korea in 2013. Currently, he is working at

Department of Electrical and Electronics Engineering, Ho Chi Minh city University of Food Industry. His research interests include power converters, machine drives, wind power generation, power quality and power system.

Nhut Minh Ho was born in Vietnam in 1987. He received his undergraduate degree in 2010, major in Electronics & Telecommunications Engineering from University of Technical Education of Ho Chi Minh City. In 2014, he received the Master of Telecommunication Engineering Degree from Posts and Telecommunications Institute of Technology, Ho Chi Minh City Campus. He is working at Department of Electrical and Electronic Engineering, Posts and Telecommunications Institute of Technology, Ho Chi Minh City Campus, VietNam.